Plant Physiol. (1989) 91, 1364–1371
0032-0889/89/91/1364/08/$01.00/0

Received for publication April 14, 1989
and in revised form June 29, 1989

CO_2 Concentrating Mechanism of C_4 Photosynthesis

Permeability of Isolated Bundle Sheath Cells to Inorganic Carbon

Robert T. Furbank, Colin L. D. Jenkins*, and Marshall D. Hatch
Division of Plant Industry, CSIRO, P. O. Box 1600, Canberra City 2601 ACT, Australia

ABSTRACT

Diffusion of inorganic carbon into isolated bundle sheath cells from a variety of C_4 species was characterized by coupling inward diffusion of CO_2 to photosynthetic carbon assimilation. The average permeability coefficient for CO_2 (P_{CO_2}) for five representatives from the three decarboxylation types was approximately 20 micromoles per minute per milligram chlorophyll per millimolar, on a leaf chlorophyll basis. The average value for the NAD-ME species *Panicum miliaceum* (10 determinations) was 26 with a standard deviation of 6 micromoles per minute per milligram chlorophyll per millimolar, on a leaf chlorophyll basis. A P_{CO_2} of at least 500 micromoles per minute per milligram chlorophyll per millimolar was determined for cells isolated from the C_3 plant *Xanthium strumarium*. It is concluded that bundle sheath cells are one to two orders of magnitude less permeable to CO_2 than C_3 photosynthetic cells. These data also suggest that CO_2 diffusion in bundle sheath cells may be made up of two components, one involving an apoplastic path and the other a symplastic (plasmodesmatal) path, each contributing approximately equally.

Central to the operation of C_4 photosynthesis is a process that concentrates CO_2 in the bundle sheath cells to levels probably in excess of 20 times atmospheric concentrations (11, 12). The resulting suppression of photorespiration and increase in CO_2 assimilation is responsible for the improved photosynthetic performance of C_4 plants compared with C_3 plants (13, 15). The CO_2 concentrating function of C_4 photosynthesis is only possible if there is a relatively high resistance to diffusion of inorganic carbon, and in particular CO_2, out of the bundle sheath cells compared to that prevailing for other photosynthetic cells (13). It has been suggested that this increased resistance may be due to the suberised lamellae or similar structures found in the cell wall separating mesophyll and bundle sheath cells of most C_4 species (13, 15). The leakiness to CO_2 of this diffusion barrier is an important determinant in the efficiency of C_4 photosynthesis; the greater the diffusive loss of CO_2 from the bundle sheath cell compartment, the more energy must be expended to operate the C_4 acid cycle that generates CO_2 in that compartment (7, 15).

Bundle sheath cells isolated from several C_4 species are highly permeable to a variety of small mol wt compounds, as judged by consequent metabolic responses (3, 4, 14, 22, 28). Recent studies on the diffusion of various metabolites into isolated bundle sheath cells led to the conclusion that these compounds move via plasmodesmatal pores located in the bundle sheath cell walls (28). Clearly, inorganic carbon (CO_2 + HCO_3^-) could diffuse via this symplastic path and by apoplastic diffusion of the uncharged species CO_2 through the cell wall. As indicated above, the degree of permeability of bundle sheath cells to CO_2 is critical in the operation of C_4 photosynthesis but to date no measurements of this parameter are available. This information would also be critical to the sophistication of a model developed previously (11) to predict the size and composition of the bundle sheath cell inorganic carbon pool. A substantially refined version of this model is presented in an accompanying paper (17).

In the present study we examine the permeability of isolated bundle sheath cells to inorganic carbon by measuring photosynthetic O_2 evolution or CO_2 fixation in response to adding limiting levels of inorganic carbon to the assay medium. Permeability coefficients for the flux of CO_2 into the bundle sheath cells were calculated for a number of C_4 species and for cells from a C_3 species.

MATERIALS AND METHODS

Materials

Plants were grown in soil, naturally illuminated in a glasshouse maintained at 20 to 30°C. Biochemicals and reagents were obtained from Boehringer-Mannheim, Australia or Sigma Chemical Company. RuBP,[1] prepared from ribose 5-phosphate, was a kind gift from M. R. Badger.

Preparation of Bundle Sheath Cell Strands

Bundle sheath cell strands free of mesophyll tissue were prepared mechanically essentially as described by Weiner *et al.* (28) except that homogenization and resuspension media were gassed with N_2 at pH 5 to remove residual inorganic carbon prior to adjusting to pH 7.5 with freshly prepared KOH.

Preparation of *Xanthium* Cells

Intact cells of *Xanthium strumarium* were isolated mechanically according to Sharkey and Raschke (24). The cells were resuspended in CO_2-free isolation buffer (0.1 M Hepes-KOH, pH 7) and bubbled gently with CO_2-free air during storage at room temperature.

[1] Abbreviations: RuBP, ribulose 1,5-bisphosphate; Rubisco, ribulose 1,5-bisphosphate carboxylase/oxygenase.

Measurement of Photosynthetic Oxygen Evolution

Light and CO_2-dependent O_2 evolution by isolated cells was measured polarographically using a Rank Bros. (Cambridge, U.K.) oxygen electrode. Reactions were run in CO_2-free buffer (0.3 M sorbitol, 20 mM Hepes-KOH [pH 7.5], 0.5 mM Pi, and 10 mM KCl for bundle sheath cells and the isolation buffer for *Xanthium* cells) and gassed with nitrogen to give a final O_2 concentration of 100 to 150 μM. The Chl concentration varied between 10 and 25 μg/mL in a 2 mL assay volume. Assays were conducted at 30°C with an incident irradiance of 3000 μmol quanta m^{-2} s^{-1} (white light provided by a quartz iodide slide projector) unless indicated otherwise. In the absence of added inorganic carbon, no light-dependent O_2 evolution was evident either with *Xanthium* cells or bundle sheath cells.

Measurement of Photosynthetic $^{14}CO_2$ Fixation

Measurements of $^{14}CO_2$ incorporation were made in the O_2 electrode cuvette essentially as described above except that $NaH^{14}CO_3$ (2.18 MBq/mmol, 10 μL of 6.8 mM, per 2 mL reaction) was added after a steady state of O_2 evolution was achieved in the presence of unlabeled CO_2. The cuvette lid was removed and samples (0.5 mL) withdrawn at 30 s intervals over a 2 min period. These samples were injected into 0.1 mL trifluroacetic acid to give a final concentration of 1 M acid. After centrifugation, samples of the supernatant were evaporated to dryness under a stream of air. Acid stable $^{14}CO_2$ incorporation was determined by scintillation counting. The specific activity of CO_2 in each reaction was individually determined by injecting a sample into 30% hyamine hydroxide in ethanol for the determination of total ^{14}C.

Transient Kinetics of $^{14}CO_2$ or $H^{14}CO_3$ Incorporation

The time-course of ^{14}C incorporation was followed after the addition of either $^{14}CO_2$ or $NaH^{14}CO_3$. This was done by adding either 10 μL stock $NaH^{14}CO_3$ prepared in 10 mM NaOH (>99.9% HCO_3^-) or in 10 mM HCl (>99% CO_2) to a 5 mL reaction containing bundle sheath cells which had been preilluminated with 0.5 mM inorganic carbon (CO_2 plus HCO_3^- in equilibrium) for 2 min. Samples (0.75 mL) were removed at short intervals and quenched in 0.5 mL of 1 M NaOH. Reactions were illuminated at 3000 μmol quanta m^{-2} s^{-1} and this level of irradiance was maintained up to the instant of transfer of NaOH. After centrifugation, the subsamples were acidified and treated for scintillation counting as described above.

Rubisco Assays and Activation State

Rubisco activity in bundle sheath cells was assayed by two methods. For estimations of V_{max}, 3 mL of cells were centrifuged out of the resuspension medium and vigorously ground for 1 min in a mortar at 0°C in Rubisco assay medium (50 mM tricine [pH 8.3] and 20 mM $MgCl_2$). The homogenate was filtered through Miracloth and 0.5 mL of the filtrate transferred to a temperature controlled cuvette (30°C). The remaining filtrate was retained for Chl estimation (29). $NaHCO_3$ was then added (final concentration 10 mM) and the mixture incubated for 2 min to fully activate the enzyme (further incubation gave no increase in activity). $NaH^{14}CO_3$ (10 μL of stock) was then added and the reaction initiated by the addition of 0.5 mM RuBP. Acid stable ^{14}C incorporation was determined in aliquots removed at 10, 20, and 30 s as described above.

For determinations of Rubisco activation state, a 2 mL sample of bundle sheath cells was removed from the O_2 electrode cuvette after incubation under the standard assay conditions and the cells were rapidly collected on a filter paper under vacuum in a millipore apparatus. Liquid nitrogen was then poured over the cells which were ground to a fine powder in a mortar precooled to liquid nitrogen temperature. The entire procedure was carried out under illumination (approximately 1000 μmol quanta m^{-2} s^{-2} white light) and the time between removal of the sample and freezing was less than 5 s. Samples of the powder were transferred to Rubisco assay medium and immediately assayed for activity. Microscopic examination of the treated samples showed that no chloroplasts or cells remained. When fully activated, samples prepared in this way gave similar activities to those prepared by grinding bundle sheath cells in a mortar at 0°C.

Xanthium cells were extracted for Rubisco assays by resuspending in Rubisco assay medium containing 5 mM DTT and 1% PVP 40 and grinding in a mortar in liquid nitrogen. Some of the frozen powder was then transferred to standard Rubisco medium and assayed as described above. Rubisco V_{max} values obtained agreed well with those determined for the same leaf tissue after liquid nitrogen treatment according to Fischer *et al.* (9).

Carbonic Anhydrase Assays

Leaves of *Panicum miliaceum* were extracted by grinding at 0°C in a mortar in a medium containing 50 mM Hepes-KOH (pH 7.5), 5 mM $MgCl_2$, and 5 mM DTT. The assays were performed at 0°C as described by Burnell and Hatch (3).

RESULTS AND DISCUSSION

Bundle Sheath Cell Permeability to CO_2 and HCO_3^-

A technique for distinguishing between CO_2 and HCO_3^- uptake into algal cells, plant cells, protoplasts, and chloroplasts is to measure the transient kinetics of ^{14}C incorporation after adding inorganic carbon to the preparation either as $H^{14}CO_3$ or $^{14}CO_2$ (2, 27). This technique relies upon a relatively slow equilibration of CO_2 and HCO_3^- in the medium with carbonic anhydrase absent (or inhibited). This slow equilibration allows time-courses for ^{14}C fixation from either $^{14}CO_2$ or $H^{14}CO_3$ to be generated before these species become fully equilibrated with the unlabeled inorganic carbon pool. In some of the following experiments ethoxyzolamide, an inhibitor of carbonic anhydrase (23), was added to eliminate that component of CO_2 and HCO_3^- interconversion due to traces of carbonic anhydrase released into the medium or located within the bundle sheath cells (which normally have very low activities of this enzyme; see ref. 3). Ethoxyzolamide was found to strongly inhibit carbonic anhydrase from *Panicum miliaceum* leaves ($I_{50} < 1$ μM, data not shown).

In Figure 1, either $H^{14}CO_3^-$ or $^{14}CO_2$ was added to a reaction mixture after bundle sheath cells had reached a steady rate of photosynthesis in the presence of 0.5 mM unlabeled inorganic carbon and the time-course of incorporation followed. Figure 2 provides a model description of this system with kinetic parameters at photosynthetic steady-state. The values indicated on the diagram are for the condition where there is no carbonic anhydrase activity in either the medium or the cells. With added carbonic anhydrase, ^{14}C incorporation remained constant over the 20 s period with either labeled substrate (Fig. 1, A and B) presumably due to the very rapid equilibration of the CO_2 and HCO_3^- pools. In the absence of added carbonic anhydrase, ^{14}C incorporation from $H^{14}CO_3^-$ was slow initially but accelerated with time while incorporation from $^{14}CO_2$ was rapid initially but declined; these effects were more pronounced in the presence of ethoxyzolamide.

These results suggest that the carbon assimilated in the cells is provided predominantly or solely by the flux of CO_2 as such. As observed, incorporation of label from $^{14}CO_2$ should decline as the radioactivity in the small CO_2 pool is progressively diluted by exchange with the large HCO_3^- pool (about 94% of total inorganic carbon at pH 7.5, see Fig. 2). Likewise, ^{14}C incorporation from $H^{14}CO_3^-$ would accelerate as the specific activity of the CO_2 pool increases. Notably, the ^{14}C incorporation from added $H^{14}CO_3^-$ in the control and the plus ethoxyzolamide treatments never reached the steady-state rates achieved in the presence of carbonic anhydrase (Fig. 1A). This was presumably attributable to limitation of photosynthesis imposed by the rate of conversion of HCO_3^- to CO_2 in the medium and an associated lower steady-state level of CO_2 (Fig. 2).

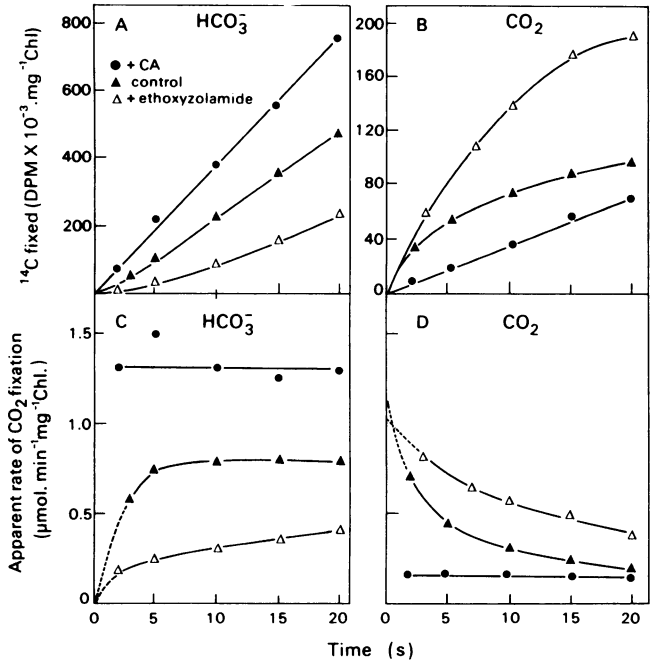

Figure 1. Time course of ^{14}C incorporation by bundle sheath cells of *P. miliaceum* from added $H^{14}CO_3^-$ (A) or $^{14}CO_2$ (B). Carbonic anhydrase (0.2 mg mL$^-$) or ethoxyzolamide (25 μM) were added as indicated. C and D show this data replotted as a rate of CO_2 assimilation (CO_2 fixed divided by the time elapsed after ^{14}C addition) based on the initial specific activity of the inorganic carbon added (see text for details). Rates of photosynthesis at steady-state were 1.3 μmol min^{-1} (mg Chl)$^{-1}$ with carbonic anhydrase present, 1.2 in the control and 0.9 with ethoxyzolamide present.

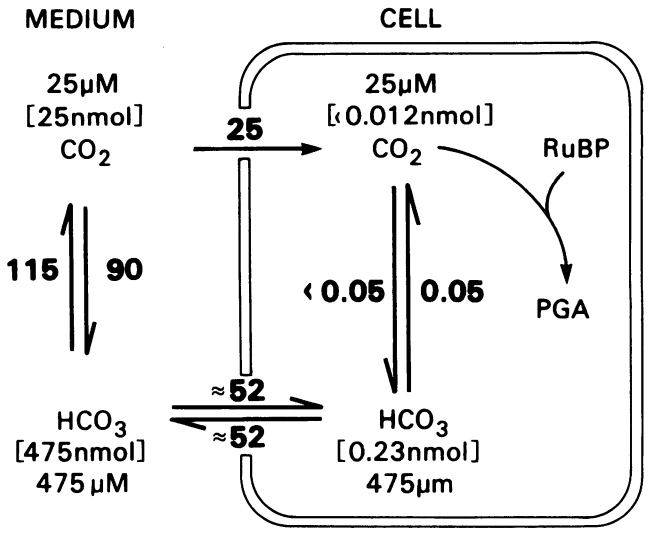

Figure 2. Model showing the relationships between the inorganic carbon pools of isolated bundle sheath cells and the suspending medium. The diagram shows the approximate pool sizes, concentrations and velocities for CO_2 and HCO_3^- interconversion (nmol mL^{-1} of reaction) during steady-state photosynthesis under the following conditions: reaction mixtures of 1 mL volume containing cells equivalent to 20 μg Chl, 500 μM total inorganic carbon (and assuming pH 7.5 in the medium and the cytosol of the cells) and a photosynthetic rate of 1.25 μmol min^{-1} (mg Chl)$^{-1}$. It is also assumed that there is no carbonic anhydrase in either the medium or the cytosol. The rate constants for the spontaneous interconversion of CO_2 to HCO_3^- and HCO_3^- to CO_2 are taken as 6×10^{-2} s^{-1} and 4×10^{-3} s^{-1}, respectively (11). At thermodynamic equilibrium the concentrations of CO_2 and HCO_3^- with 0.5 mM total inorganic carbon would be 27 and 473 μM, respectively.

In Figure 1, C and D, the data from Figure 1, A and B, are presented as the apparent rate of carbon assimilation assuming a specific activity equivalent to that prevailing at the instant $^{14}CO_2$ or $H^{14}CO_3^-$ were added. Extrapolation of these curves to zero time provides an estimate of the initial rate of carbon incorporation from CO_2 or HCO_3^-, providing interconversion is limited. Particularly in the presence of ethoxyzolamide the curves for $H^{14}CO_3^-$ extrapolated toward zero while the curve with $^{14}CO_2$ added gave apparent initial rates very close to the steady state rate of CO_2 incorporation (measured independently by the addition of $H^{14}CO_3 + {}^{14}CO_2$ at equilibrium, see legend to Fig. 1). Bicarbonate probably rapidly penetrates bundle sheath cells (28) but it is very unlikely to enter chloroplasts at significant rates (27). Even if HCO_3^- penetrated the chloroplast, it may still provide little of the carbon for photosynthesis if the rate of conversion of HCO_3^- to CO_2 is limited in the absence of carbonic anhydrase.

Measurement of CO_2 Diffusion into Bundle Sheath Cells

The results presented above indicate that CO_2 diffusion into bundle sheath cells might be studied by measuring photosyn-

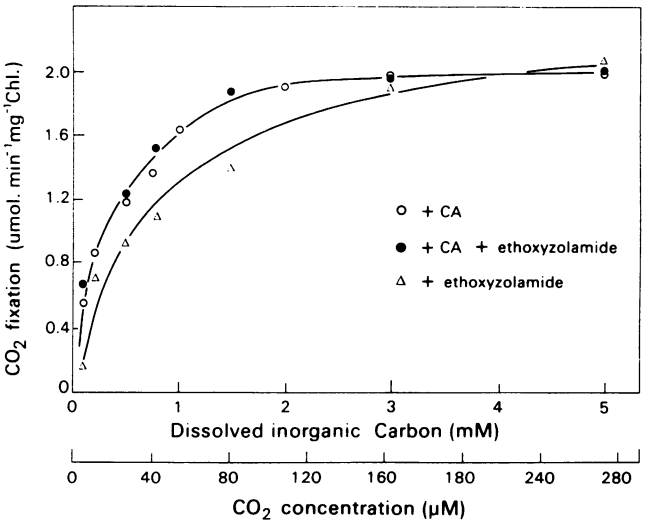

Figure 3. Response of photosynthesis in bundle sheath cells from *P. miliaceum* to added inorganic carbon at saturating light in the presence of carbonic anhydrase (0.2 mg·ml^{-1}), ethoxyzolamide (5 μM) or both carbonic anhydrase and ethoxyzolamide. Photosynthesis was measured as CO_2 assimilation by $^{14}CO_2$ incorporation. The CO_2 concentration in the medium, assuming equilibrium at pH 7.5, is also shown on the X-axis.

thesis at limiting inorganic carbon concentrations. Figure 3 shows the effect of varying inorganic carbon concentration on carbon assimilation in bundle sheath cells in reactions supplemented with either carbonic anhydrase or ethoxyzolamide separately or together. Carbonic anhydrase was added to ensure that conversion of HCO_3^- to CO_2 in the medium was not limiting photosynthesis (see above). Ethoxyzolamide was added to inhibit any cell carbonic anhydrase although, when added alone, it would eliminate any carbonic anhydrase activity remaining in the medium. Where carbonic anhydrase was added with ethoxyzolamide, trials showed that in spite of substantial inhibition, the remaining activity in the medium (>500 times the uncatalysed rate) was sufficient to ensure that HCO_3^- conversion to CO_2 did not limit photosynthesis.

Photosynthesis was saturated at about 2 mM inorganic carbon with carbonic anhydrase alone and between 3 and 5 mM with ethoxyzolamide alone (Fig. 3). Ethoxyzolamide inhibited photosynthesis up to 75% with low levels of added inorganic carbon but had no effect with 3 mM inorganic carbon or more. Inclusion of carbonic anhydrase with ethoxyzolamide completely prevented this inhibition of photosynthetic activity (Fig. 3). This effect of ethoxyzolamide was similar to that seen in the experiments shown in Figure 1 where 0.5 mM inorganic carbon was used. Both sets of data are best interpreted in terms of ethoxyzolamide inhibiting traces of carbonic anhydrase in the medium so that the remaining uncatalysed rate of conversion of HCO_3^- to CO_2 is too low to maintain maximum rates of photosynthesis (see Fig. 2). These results also support the view that carbonic anhydrase within the bundle sheath cells, which would also be inhibited by ethoxyzolamide, does not contribute significantly to the provision of CO_2 internally from HCO_3^-. We concluded from these studies that, especially in the presence of carbonic anhydrase, photosynthesis provides an accurate measure of CO_2 flux into these cells.

Calculation of Permeability Coefficients for CO_2

It is possible to calculate the permeability coefficient for CO_2 diffusion into bundle sheath cells from the data in Figure 3, provided the internal $[CO_2]$ can be determined by measuring Rubisco activity and its K_mCO_2. The permeability coefficient (P) is defined as a CO_2 flux per unit gradient:

$$P = \frac{v}{[CO_2]_{OUT} - [CO_2]_{IN}} \quad (1)$$

where $[CO_2]_{OUT}$ is the CO_2 concentration in the medium (calculated from the Henderson-Hasselbach equation and a pK′ of 6.23, assuming an ionic strength of 20 mM in the reaction medium [31]), $[CO_2]_{IN}$ is the internal CO_2 concentration within the chloroplast (both in mM units), and v is the CO_2 flux, measured as the rate of photosynthesis in μmol min^{-1} (mg Chl)$^{-1}$ (assuming the contribution of HCO_3^- is insignificant). This coefficient is equivalent to the permeability coefficient defined by Nobel (21). P in this study has the units μmol min^{-1} (mg Chl)$^{-1}$ mM^{-1} [as used previously (28)]. Expression of P in these units is appropriate for the present study but they can be converted to cm s^{-1} (the units more commonly used in biophysics) providing the area of bundle sheath cells per unit Chl is known (see below).

When CO_2 limits photosynthesis, the internal CO_2 can be calculated from the rate of photosynthesis, the kinetic parameters of the Rubisco for the species used, the V_{max} of the Rubisco *in vivo*, and an assumed O_2 concentration. These parameters are related by the following equation:

$$v = \frac{V_{max}[CO_2]_{IN}}{[CO_2]_{IN} + K_c(1 + [O_2]/K_o)} \quad (2)$$

where v and $[CO_2]_{IN}$ are as defined in Equation 1, K_c is the K_m for CO_2 of the Rubisco, K_o the inhibition constant for O_2 for Rubisco, and $[O_2]$ the oxygen concentration. The parameter v is easily measured and there are published values for K_c and K_o for Rubisco from various C_4 species (18, 30). Where applicable these published K_c values were corrected by using a pK′ value appropriate to high ionic strength buffer (pK′ 6.12 for 100 mM monovalent buffer; see ref. 31). This reduces reported K_c values considerably (*e.g.* a K_c value of 58 μM [30] corrects to 32 μM).

To apply Equation 2 it must be assumed that the rate of photosynthesis at limiting CO_2 is entirely dependent upon the prevailing potential Rubisco activity (*i.e.* the enzyme *in situ* is fully activated and RuBP saturated). To establish that Rubisco was fully activated in bundle sheath cells, the activation state of Rubisco at saturating light and 0.5 mM inorganic carbon was determined (see "Materials and Methods"). With *P. miliaceum* cells, the average activity for three separate experiments was 12.5 ± 2 μmol min^{-1} (mg Chl)$^{-1}$ in freshly isolated extracts and 11.5 ± 1.5 μmol min^{-1} (mg Chl)$^{-1}$ after treatment to fully activate the enzyme.

Evidence for RuBP saturation of the enzyme in isolated bundle sheath cells was provided by comparing photosynthetic flux at 3000 μmol quanta m^{-2} s^{-1} (the standard incident

irradiance) and 800 μmol quanta m^{-2} s^{-1} in the presence of 0.5 or 5 mM inorganic carbon (Table I). With illumination of cells at the lower light intensity in the presence of 5 mM inorganic carbon the rate of photosynthesis was reduced by over 50%. However, this low light intensity remained saturating with 0.5 mM inorganic carbon as determined either by illumination of cells from time zero at different light levels or when given a step change in light intensity from 800 to 3000 μmol quanta m^{-2} s^{-1} was made. This indicates that while the rate of RuBP regeneration at saturating inorganic carbon is limiting when the light is reduced to 800 μmol quanta m^{-2} s^{-1}, this irradiance is still sufficient to saturate the Rubisco with RuBP at the lower CO_2 concentration. Clearly, the potential capacity for RuBP regeneration at high light and low CO_2 would substantially exceed the observed rate of photosynthesis.

Another kinetic parameter which is required for calculation of $[CO_2]_{IN}$ is the true potential V_{max} of Rubisco in bundle sheath cells. The V_{max} for photosynthesis of bundle sheath cells with optimal light and CO_2 underestimates the true V_{max} for Rubisco, presumably due to a limitation imposed by the light dependent rate of RuBP regeneration (8). Such a limitation would account for the abrupt plateauing of CO_2 response curves seen here and elsewhere (Figs. 3 and 4; Refs. 8, 10). The V_{max} of Rubisco was therefore determined in each experiment by assaying the extracted enzyme at saturating CO_2 and RuBP.

A minimum value for the diffusion of O_2 from bundle sheath cells can be derived from the P value for C_4 acids (found to be about 9 μmol min^{-1} [mg Chl]$^{-1}$ mM^{-1} for *P. miliaceum* bundle sheath cells; ref. 28]. If we assume that at least this path is available for O_2 diffusion and that O_2 diffuses 4.1 times faster than C_4 acids (based on differences in diffusion coefficients [15]), then an approximate P_{O_2} would be around 36 μmol min^{-1} (mg Chl)$^{-1}$ mM^{-1} or greater. For an external O_2 concentration of 230 μM (air O_2 in equilibrium with water at 30°C), we can calculate from Equation 1 internal $[O_2]$ values of 260 to 370 μM for photosynthetic rates of 1 and 5 μmol min^{-1} (mg Chl)$^{-1}$, respectively.

Table I. *Effect of Light Intensity on CO_2 Incorporation by P. miliaceum Bundle Sheath Cells*

The rate of photosynthesis at two light intensities and at limiting and saturating CO_2 was measured by $^{14}CO_2$ incorporation. Reactions contained 0.2 mg/mL carbonic anhydrase. See "Materials and Methods" for further details.

Experimental Conditions	Rate of CO_2 Incorporation
	μmol min^{-1} (mg Chl)$^{-1}$
5 mM inorganic carbon, 3000 μmol quanta m^{-2} s^{-1}	1.8
5 mM inorganic carbon, 800 μmol quanta m^{-2} s^{-1}	0.86
0.5 mM inorganic carbon, 3000 μmol quanta m^{-2} s^{-1}	0.58
0.5 mM inorganic carbon, 800 μmol quanta m^{-2} s^{-1}	0.60
0.5 mM inorganic carbon, 3000 μmol quanta m^{-2} s^{-1} after 2 min at 800 μmol quanta m^{-2} s^{-1}	0.58

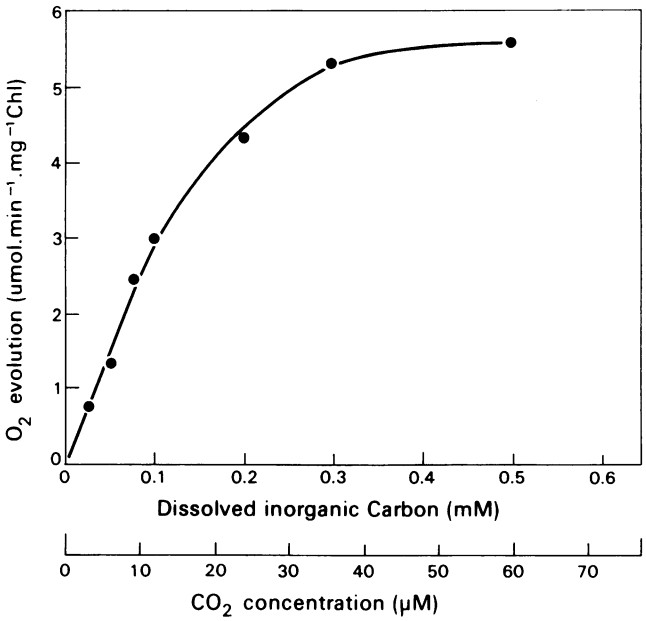

Figure 4. Response of photosynthetic O_2 evolution by isolated cells of *X. strumarium* to added inorganic carbon with saturating light. The V_{max} of Rubisco from these cells was 9.5 μmol min^{-1} (mg Chl)$^{-1}$. The CO_2 concentration in the medium assuming equilibrium at pH 7 is also shown on the X-axis.

Table II shows the P_{CO_2} values obtained from the data shown in Figure 3 using Equation 1 and $[CO_2]_{IN}$ calculated from Equation 2. The first entry in the table gives the best estimate for P_{CO_2} (49 μmol min^{-1} [mg Chl]$^{-1}$ mM^{-1}) based on the most likely values for internal O_2 concentration, K_c and the V_{max} of Rubisco (see above). Also shown is the effect on P_{CO_2} of varying these parameters. It is apparent that P is relatively insensitive to the cellular O_2 concentration due to the fact that the K_i for O_2 is quite high for C_4 Rubisco (18). By contrast, when the photosynthetic rate, K_c or V_{max} of Rubisco are arbitrarily varied by a factor of two (relative to the standard measured values), there is a larger change in the P_{CO_2} value.

CO_2 Diffusion in C_3 Cells

The apparent P_{CO_2} for CO_2 diffusion into cells isolated from the C_3 plant *Xanthium strumarium* was determined from the CO_2-photosynthesis response curve shown in Figure 4, using the procedure described above for bundle sheath cells. As carbonic anhydrase would be present in *Xanthium* cells, the P value obtained by this method would include the diffusion of both HCO_3^- and CO_2. However, as C_3 cells have been shown to be relatively impermeable to HCO_3^- (27), CO_2 diffusion would predominate. Using a value of 9.5 μmol min^{-1} (mg Chl)$^{-1}$ determined for the potential *in situ* V_{max} of Rubisco, a value of 11 μM for K_c and 480 μM for K_o (18), an internal $[O_2]$ of 230 μM and using the rate of photosynthesis at 0.05 mM inorganic carbon (1.5 μmol min^{-1} [mg Chl]$^{-1}$) as the CO_2 flux rate into the cell, we calculated P_{CO_2} to be 510

Table II. *Effect of Varying Critical Parameters on the Calculated Values of P_{CO_2}*

Permeability coefficients are calculated from the data of Figure 3 using the photosynthetic rate with 0.5 mM inorganic carbon (0.027 mM CO_2), a K_c of 0.032 mM and K_0 of 0.8 mM and presented on a bundle sheath Chl basis.

Internal $[O_2]$	$[CO_2]_{IN}$	Photosynthesis	V_{max} Rubisco	P_{CO_2}
μM	mM	μmol min^{-1} (mg Chl)$^{-1}$		μmol min^{-1} (mg Chl)$^{-1}$ mM^{-1}
260	0.004	1.12	12.8	49[a]
115	0.0035	1.12	12.8	48
480	0.005	1.12	12.8	51
260	0.009	1.12	6.4	62
260	0.002	0.65	12.8	26
260	0.002 (K_c/2)	1.12	12.8	45
260	0.008 ($K_c \times 2$)	1.12	12.8	59

[a] This value represents the best estimate of P_{CO_2} based on the most likely values for the variable parameters.

μmol min^{-1} (mg Chl)$^{-1}$ mM^{-1}. However, it should be noted that errors in determining the P_{CO_2} become large with such high permeabilities and associated diminishing differences between external and internal CO_2. Under these circumstances, the accuracy of the kinetic constants of Rubisco used in this calculation become critical. For example, if the K_c for Rubisco is assumed to be 15 μM, P_{CO_2} becomes 846 μmol min^{-1} (mg Chl)$^{-1}$ mM^{-1} and for a K_c of 20 μM, P_{CO_2} becomes 4125 μmol min^{-1} (mg Chl)$^{-1}$ mM^{-1}. The range 11 to 20 μM for K_c corresponds to the range reported in the current literature (18, 30). It is also notable that the P values obtained here for *Xanthium* cells are of the same order as those calculated from gas exchange data with intact C_3 leaves (5, 6). Expressed as a conductance, these values are around 0.42 to 0.84 mol m^{-2} s^{-1} bar^{-1} which, assuming a leaf Chl content of 400 mg m^{-2} and the solubility of CO_2 at 20°C to be 0.878 L/L (26), represents a P_{CO_2} value of between 1595 and 3189 μmol min^{-1} (mg Chl)$^{-1}$ mM^{-1}.

P_{CO_2} for Bundle Sheath Cells from Different C_4 Species

The P_{CO_2} for bundle sheath cells of a number of C_4 species was determined as described above (Table III). The values obtained ranged from 16 to 48 μmol min^{-1} (mg Chl)$^{-1}$ mM^{-1}. They are also expressed on a leaf Chl basis using data on the distribution of Chl between bundle sheath and mesophyll cells for individual species (19, 20) or, where this value was not available, using the average distribution for the decarboxylation type (20). To give some measure of the variability of these determinations of P_{CO_2}, 10 separate measurements made with *P. miliaceum* cells gave an average value of 40 (on a bundle sheath Chl basis) with a standard deviation of 13 μmol min^{-1} (mg Chl)$^{-1}$ mM^{-1}. Rubisco activity varied between preparations but ten determinations on three separate scaled-down preparations from the same plant material gave an average activity of 8.1 with a standard deviation of 1.0 μmol min^{-1} (mg Chl)$^{-1}$.

CONCLUDING COMMENTS

The present studies provide quantitative evidence to support predictions (7, 11, 13, 15) that bundle sheath cells in C_4 plants must have a very low permeability to CO_2 compared to other photosynthetic cells. The permeability coefficient for CO_2 determined here is a critical parameter in a model developed to predict the inorganic carbon status of bundle sheath cells during steady-state photosynthesis (see accompanying paper, ref. 17).

The average P_{CO_2} for bundle sheath cells from several C_4 species, determined in the present study, was approximately 20 μmol min^{-1} (mg Chl)$^{-1}$ mM^{-1} on the basis of total leaf Chl. This value is very similar to the average P_{CO_2} value determined for apparent CO_2 diffusion into the bundle sheath of intact C_4 leaves in an accompanying paper (16) and compares with an average P value of 3.5 μmol min^{-1} (mg Chl)$^{-1}$ mM^{-1} determined for the diffusion of organic acids (mol wt range 131–170) into isolated bundle sheath cells (28). It was concluded that these organic acids diffuse via plasmodesmata, large numbers of which traverse the cell wall separating mesophyll and bundle sheath cells. Assuming that the diffusive flux of organic acids and CO_2 through plasmodesmata is directly proportional to their diffusion coefficients (15) a permeability coefficient for CO_2 of 8.3 μmol min^{-1} (mg Chl)$^{-1}$ mM^{-1} can be derived. This value is less than half of the average value of about 20 μmol min^{-1} (mg Chl)$^{-1}$ mM^{-1} measured for the CO_2 permeability of bundle sheath cells in the present study. The inferred additional path for CO_2 flux may be the apoplastic route via the plasmalemma and cell wall; it is through this path that CO_2 passes very rapidly into other photosynthetic cells (see above).

The average P_{CO_2} we obtained for bundle sheath cells was between 1 and 2 orders of magnitude lower than that determined for leaf cells from the C_3 species *Xanthium*. As indicated above, our P_{CO_2} values for *Xanthium* may be minimum estimates of the CO_2 permeability of C_3 photosynthetic cells. For instance, values of P_{CO_2} in the range of 0.07 to 0.17 cm s^{-1} (calculated from ref. 5) have been obtained based on leaf

Table III. *Permeability Coefficients of CO_2 for Bundle Sheath Cells from a Range of Different C_4 Species*

The rate of CO_2 incorporation at limiting (27 μM) and saturating CO_2 was determined and the P_{CO_2} calculated from the V_{max} of Rubisco from each preparation. A value for *X. strumarium* cells is included for comparison. *P* values are expressed both on a bundle sheath Chl basis (BSC) and a leaf Chl basis. P_{CO_2} values are averages of three determinations made on a single cell preparation. All experiments contained 0.2 mg/mL carbonic anhydrase. *Z. mays* cells were provided with 5 mM dihydroxyacetone phosphate as a reduced carbon source. The kinetic constants used in the calculation of $[CO_2]_{IN}$ and *P* were as follows: K_0 for all C_4 species was taken to be 800 μM (18); O_2 concentration within the bundle sheath cells was assumed to be 260 μM with an external O_2 concentration of 150 μM in the assay; K_c for NAD-ME, NADP-ME, and PCK types were 31, 32, and 23 μM, respectively (recalculated from ref. 30); K_c for *Xanthium* was 11 μM (18). The photosynthetic rate used for the calculation of the *P* value for *Xanthium* was determined at 6 μM CO_2 as the higher CO_2 concentration was near saturation for photosynthesis with these cells. The Rubisco V_{max} was determined for each cell preparation as described in the text.

Species	Decarboxylation Type	Rates			P_{CO_2}	
		Photosynthesis		Rubisco V_{max}	BSC Chl basis	Leaf Chl basis
		CO_2 limited	CO_2 saturated			
		μmol min^{-1} (mg Chl)$^{-1}$			μmol min^{-1} (mg Chl)$^{-1}$ mM^{-1}	
Panicum miliaceum	NAD-ME	0.8	2.2	7	38	24
Atriplex spongiosa	NAD-ME	1.1	2.2	12	40	30
Urochloa panicoides	PEP-CK	0.95	4.1	13	39	27
Chloris gayana	PEP-CK	0.54	1.45	13	21	14
Zea mays	NADP-ME	0.4	1.5	11	16	6
Xanthium strumarium	C_3	2.4	5.6	9.5		510–3000[a]

[a] Range depending on assumed K_c for Rubisco (see text).

gas exchange measurements (6), carbon isotope discrimination (5), and from consideration of the individual resistances in the cell (*i.e.* cell wall, plasmalemma, cytosol [21]). If the P_{CO_2} values obtained here for bundle sheath cells are converted to these units (assuming a bundle sheath surface area of 100 cm^2 [mg leaf Chl]$^{-1}$ for monocots and 62 cm^2 [mg leaf Chl]$^{1-}$ for dicots [15]), values of between 0.0016 and 0.0045 cm s^{-1} are obtained; *i.e.* around two orders of magnitude lower than the values reported for C_3 cells. However, bundle sheath cells appear to be more permeable to CO_2 than green microalgae or cyanobacteria for which P_{CO_2} values are reported of approximately 10^{-4} and 10^{-5} to 10^{-7} cm s^{-1}, respectively (1).

ACKNOWLEDGEMENTS

R. T. Furbank was the recipient of a Queen Elizabeth II fellowship for the duration of this work.

LITERATURE CITED

1. **Badger MR** (1987) The CO_2 concentrating mechanism in aquatic phototrophs. *In* MD Hatch, NK Boardman, eds. The Biochemistry of Plants, Vol 10. Academic Press New York, pp 219–274
2. **Badger MR, Andrews TJ** (1982) Photosynthesis and inorganic carbon usage by the marine cyanobacteria, Synechococus sp. Plant Physiol **70:** 517–523
3. **Burnell JN, Hatch MD** (1988) Low bundle sheath carbonic anhydrase is apparently essential for effective C_4 pathway operation. Plant Physiol **86:** 1252–1256
4. **Chapman KSR, Berry JA, Match MD** (1980) Photosynthetic metabolism in the bundle sheath of the C_4 species *Zea mays*. Arch Bioichem Biophys **202:** 330–341
5. **Evans JR, Sharkey TD, Berry JA, Farquhar GD** (1986) Carbon isotope discrimination measured concurrently with gas exchange to investigate CO_2 diffusion in leaves of higher plants. Aust J Plant Physiol **13:** 281–292
6. **Evans JR, Terashima I** (1988) Photosynthetic characteristics of spinach leaves grown with different nitrogen treatments. Plant Cell Physiol **29:** 157–165
7. **Farquhar GD** (1983) On the nature of carbon isotope discrimination in C_4 species. Aust J Plant Physiol **10:** 205–226
8. **Farquhar GD, Caemerrer S von** (1982) Modelling of photosynthetic response to environmental conditions. *In* OL Lange, PS Nobel, CB Osmond, H Ziegler, eds, Physiological Ecology. Encyclopedia of Plant Physiology (New Series), Vol 12B. Springer-Verlag, Berlin, pp 549–587
9. **Fischer E, Faschke K, Stitt M** (1986) Effects of abscisic acid on photosynthesis in whole leaves: Changes in CO_2 assimilation, levels of carbon-reduction-cycle intermediates, and activity of ribulose 1,5-bisphosphate carboxylase. Planta **169:** 536–545
10. **Furbank RT, Badger MR, Osmond CB** (1982) Photosynthetic oxygen exchange in isolated cells and chloroplasts of C_3 plants. Plant Physiol **70:** 927–931
11. **Furbank RT, Hatch MD** (1987) Mechanism of C_4 photosynthesis. The size and composition of the inorganic carbon pool in bundle sheath cells. Plant Physiol **85:** 958–964
12. **Hatch MD** (1971) The C_4 pathway of photosynthesis: Evidence for an intermediate pool of carbon dixoide and the identity of the donor C_4 acid. Biochem J **125:** 425–432
13. **Hatch MD** (1987) C_4 photosynthesis: a unique blend of modified biochemistry, anatomy and ultrastructure. Biochim Biophys Acta **895:** 81–106
14. **Hatch MD, Kagawa T** (1976) Photosynthetic activities of isolated bundle sheath cells in relation to differing mechanisms of C_4 pathway photosynthesis. Arch Biochem Biophys **175:** 39–53
15. **Hatch MD, Osmond CB** (1976) Compartmentation and transport in C_4 photosynthesis. *In* CR Stocking, U Heber, eds, Transport in Plants III. Intracellular Interaction and Transport

Processes. Encyclopedia of Plant Physiology (New Series), Vol. 3. Springer-Verlag, Berlin, pp 144–184
16. **Jenkins CLD, Furbank RT, Hatch MD** (1989) Inorganic carbon diffusion between C_4 mesophyll and bundle sheath cells: direct bundle sheath CO_2 assimilation in intact leaves in the presence of an inhibitor of the C_4 pathway. Plant Physiol **91:** 1356–1363
17. **Jenkins CLD, Furbank RT, Hatch MD** (1989) Mechanism of C_4 photosynthesis: a model describing the inorganic carbon pool in bundle sheath cells. Plant Physiol **91:** 1372–1381
18. **Jordan DB, Ogren WL** (1983) Species variation in kinetic properties of ribulose 1,5-bisphosphate carboxylase/oxygenase. Arch Biochem Biophys **227:** 425–433
19. **Ku SB, Gutierrez M, Kanai R, Edwards GE** (1974) Photosynthesis in mesophyll protoplasts and bundle sheath cells of various types of C_4 plants. II. Chlorophyll and Hill reaction studies. Z Pflanzenphysiol **72:** 320–337
20. **Mayne BC, Dee AM, Edwards GE** (1974) Photosynthesis in mesophyll protoplasts and bundle sheath cells of various types of C_4 plants. III. Fluorescence emission spectra, Delayed light emission and P700 content. Z Pflanzenphysiol **74:** 275–291
21. **Nobel PS** (1974) Introduction to Biophysical Plant Physiology. Freeman, San Francisco
22. **Rathnam CK, Edwards GE** (1977) C_4 acid decarboxlation and CO_2 donation to photosynthesis in bundle sheath strands and chloroplasts from species representing three groups of C_4 plants. Arch Biochem Biophys **182:** 1–13
23. **Reed ML, Graham D** (1980) Carbonic anhydrase in plants: distribution, properties and possible physiological roles. *In* L Reinhold, JB Harborne, T Swaine, eds, Progress in Phytochemistry, Vol 7. Pergamon Press, Oxford, pp 47–84
24. **Sharkey TD, Raschke K** (1980) Effects of phaseic acid and dihydrophaseic acid on stomata and the photosynthetic apparatus. Plant Physiol **65:** 291–297
25. Deleted in proof
26. **Umbreit WW, Burris RH, Stauffer JF** (1964) Manometric Techniques, Ed 4. Burgess Publishing Co., Minneapolis
27. **Volokita M, Kaplan A, Reinhold L** (1983) Nature of the rate limiting step in the supply of inorganic carbon for photosynthesis in isolated Asparagus mesophyll cells. Plant Physiol **72:** 886–890
28. **Weiner H, Burnell JN, Woodrow IE, Heldt HW, Hatch MD** (1988) Metabolite diffusion into bundle sheath cells from C_4 plants: relation to photosynthesis and plasmodesmatal function. Plant Physiol **88:** 815–822
29. **Wintermans JFGM, De mots A** (1965) Spectrophotometric characteristics of chlorophyll and their pheophytins in ethanol. Biochim Biophys Acta **104:** 448–453
30. **Yeoh HY, Hattersley P** (1985) K_m (CO_2) values of ribulose-1,5-bisphosphate carboxylase in grasses of different C_4 type. Phytochemistry **24:** 2277–2279
31. **Yokota A, Kitaoka S** (1985) Correct pK values for dissociation constants of carbonic acid lower the reported K_m values of ribulose bisphosphate carboxylase to half. Presentation of a nomograph and an equation for determining the pK values. Biochem Biophys Res Comm **131:** 1075–1079